



Mid to Late Holocene moisture evolution of semi-arid Mongolia and its anti-phase relationship with monsoonal Asia

Marcel Bliedtner ^{a,*}, Paul Strobel ^a, Julian Struck ^a, Maximilian Prochnow ^a,
Enkhtuya Bazarradnaa ^b, Roland Zech ^a

^a Institute of Geography, Friedrich Schiller University Jena, 07743, Jena, Germany

^b Institute of Plant and Agricultural Sciences, Mongolian University of Life Sciences, 45047, Darkhan, Mongolia

ARTICLE INFO

Article history:

Received 16 April 2023

Received in revised form

23 June 2023

Accepted 23 June 2023

Available online 30 June 2023

Handling Editor: P Rioual

Keywords:

Lake sediments

Compound-specific $\delta^2\text{H}$

Paleoclimate

Westerlies

Asian Summer Monsoon

ABSTRACT

The spatial and temporal interaction of the Westerlies and the Asian Summer Monsoon (ASM) are often suggested to drive the Holocene moisture evolution of semi-arid Mongolia and Central Asia, but so far, it has remained a controversial topic of debate. In this context, we established a high-resolution 7.4 cal ka paleohydrological record from Shireet Naiman Nuur in the central Mongolian Khangai Mountains using compound-specific biomarker $\delta^2\text{H}$ analyses. Our results suggest that drier conditions from 7.4 to 3.6 cal ka BP and wetter conditions since 3.6 cal ka BP until present are indeed related to changes in atmospheric circulation pattern. A strong anti-phasing between our record and records in monsoonal Asia shows that ASM intensification during the Mid Holocene shifted the ASM limit and adjacent subsidence dry-zones northwards, leading to increased dryness at Shireet Naiman Nuur. Overall wetter conditions during the Late Holocene are related to negative North Atlantic Oscillation phases advecting moisture into central Mongolia and Shireet Naiman Nuur by southerly-displaced Westerlies.

© 2023 The Authors. Published by Elsevier Ltd. This is an open access article under the CC BY license (<http://creativecommons.org/licenses/by/4.0/>).

1. Introduction

Semi-arid regions are expected to increasingly suffer from climate and environmental changes during the upcoming decades with severe socio-economic consequences (IPCC, 2021). Already now, semi-arid Mongolia, for example, experiences rising temperatures, longer and intensified drought conditions and changing precipitation pattern, which are predicted to intensify and become modified even further in the next decades (Marin, 2010; Hessler et al., 2018; Nanzad et al., 2021). This climate sensitivity of semi-arid Mongolia is mainly due to its continentality and complex climate forcing mechanisms that influence moisture advection and precipitation availability (D'Arrigo et al., 2000; Aizen et al., 2001). While the cold and dry winter climate is driven by the Siberian High, moisture and precipitation is mainly brought during the short summer months by the mid-latitude Westerlies (Hoerling et al., 2001; Mohtadi et al., 2016). During the past, it has been suggested that also the low-latitude Asian Summer Monsoon (ASM) played a role for moisture supply in the region to a certain degree

(Gunin et al., 1999; Chen et al., 2008; Rudaya et al., 2009). However, the evolution of these major circulation systems has been controversially discussed and there is only little consensus about their spatial interactions, particularly how they influence climate variability and moisture availability in the region. Existing paleoclimate studies from Mongolia, which are mostly based on pollen analyses, often suggest a wetting trend during the Early Holocene, dry conditions during the Mid Holocene and wet conditions again during the Late Holocene (see reviews of Wang and Feng, 2013 and Klinge and Sauer, 2019). Some authors argue that wetter conditions during the Early Holocene can be attributed to increased precipitation availability from the ASM, whereas the influence of the Westerlies started to increase during the Mid Holocene (Gunin et al., 1999; An et al., 2008; Chen et al., 2008; Rudaya et al., 2009). However, the direct influence of ASM-related precipitation to the overall proposed wet/dry/wet trend throughout the Holocene is still subject of controversy and the paleoclimate picture remains unclear. To some degree, this is because major environmental shifts often differ in their timing from site to site, which is partly due to poor chronological control, and most studies so far have used rather indirect hydrological proxies, such as pollen, sedimentological or geochemical proxies (e.g., Prokopenko et al., 2007; Sun et al., 2013;

* Corresponding author.

E-mail address: marcel.bliedtner@uni-jena.de (M. Bliedtner).

Unkelbach et al., 2019). Additionally, the paleoclimate evolution of semi-arid Central Asia, including Mongolia, has been recently the subject of an intense debate whether it is anti-phasic compared to the regions within the margins of the ASM (Zhang and Feng, 2018; Chen et al., 2019; Xu et al., 2019), but the atmospheric forcing mechanism, i.e., the spatial and temporal interaction of the Westerlies and the ASM, remains unclear so far.

For investigating past hydrological changes and moisture availability in semi-arid Mongolia, we recently proposed a novel and direct hydrological proxy which is based on the compound-specific hydrogen isotopic composition ($\delta^2\text{H}$) of *n*-alkane biomarkers in lake sediments (Bliedtner et al., 2021; Strobel et al., 2022). *n*-Alkanes comprised in lake sediments are a mixture of terrestrial and aquatic sources, and their primary hydrogen source is the environmental water used for biosynthesis (Sachse et al., 2004; Xia et al., 2008; Strobel et al., 2022). Terrestrial *n*-alkanes (e.g., *n*-C₃₁) are produced as the leaf waxes of terrestrial plants and primarily incorporate the $\delta^2\text{H}$ signal of the growing season precipitation (Sachse et al., 2012; Struck et al., 2020a, 2020b). In contrast, aquatic *n*-alkanes (e.g., *n*-C₂₃) are produced by algae and aquatic macrophytes which incorporate the $\delta^2\text{H}$ signal of lake water (Ficken et al., 2000; Sachse et al., 2004; Strobel et al., 2021, 2022). For semi-arid Mongolia, we showed in a calibration study of lake surface sediments from Khar Nuur (Nuur = lake) that the terrestrial $\delta^2\text{H}$ signal reflect very well the local growing season precipitation (Strobel et al., 2022). In contrast, the aquatic $\delta^2\text{H}$ signal is strongly enriched in the endorheic Khar Nuur, indicating that lake water is strongly modulated by evaporation. Consequently, the isotopic offset between aquatic and terrestrial $\delta^2\text{H}$, which can be expressed as $\Delta_{\text{aq-terr}}$, is a valuable indicator for lake water evaporation and therefore past hydrological changes in the lake catchment (Strobel et al., 2022). The $\Delta_{\text{aq-terr}}$ has previously been applied as a valuable hydrological proxy at high-elevation sites in Central Asia (Aichner et al., 2019; Mügler et al., 2008), and we recently used the $\Delta_{\text{aq-terr}}$ for reconstructing hydrological changes of the past 4.2 ka in the Khar Nuur sediments from the Mongolian Altai (Bliedtner et al., 2021).

Here we reconstruct Mid to Late Holocene hydrological changes from the central Mongolian Khangai Mountains based on a high-resolution biomarker isotope record. Specifically, we analyzed

compound-specific $\delta^2\text{H}$ of aquatic and terrestrial *n*-alkanes from the lake sediments of Shireet Naiman Nuur, an endorheic high-elevation lake (2429 m a.s.l.) in the Khangai Mountains previously described in detail by Bliedtner et al. (2022) for its chronostratigraphy. The lake sediments provide a good age control spanning the past 7.4 ± 0.3 cal ka BP. Within this study we aim at i) establishing a high-resolution biomarker $\delta^2\text{H}$ record for reconstructing past hydrological changes and ii) identifying and disentangling the drivers of hydrological changes for a more comprehensive understanding of the Mid to Late Holocene moisture evolution of the region.

2. Materials and methods

2.1. Study area

Shireet Naiman Nuur is located in the southeastern part of the central Mongolian Khangai Mountains ($46^\circ 31' 55.04''\text{N}$, $101^\circ 49' 16.23''\text{E}$; Fig. 1a) at high elevation (2429 m a.s.l.) in the upper Orkhon Valley. The small hydrological catchment (~ 32.5 km²) of the lake has steep slopes and reached an elevation up to ~ 3100 m a.s.l. Currently, the lake has no outlet, i.e., it is endorheic, and is therefore highly sensitive to changes in precipitation/evaporation. However, a lake level rise of ~ 5 m would result in an overspill into the upper Orkhon Valley, which could potentially have occurred during the Late Glacial due to increased meltwater inflow (Bliedtner et al., 2022). Today's mean annual temperature and precipitation at the nearest climate station Arvaikheer (CSC-ID 44388) is 2.0 ± 0.9 °C and 256.4 ± 75.2 mm, respectively, with $\sim 75\%$ of the annual precipitation falling during the summer months, i.e., June to August (period from 2009 to 2017; DWD Climate Center, 2021, Fig. 1b). Since Shireet Naiman Nuur is located ~ 600 m higher than the climate station at Arvaikheer, even lower mean annual temperatures can be expected, which ultimately lead to an ice coverage of the lake for 7 months per year (2018–2020; Planet Team, 2017). The modeled hydrogen isotopic composition of precipitation at Shireet Naiman Nuur is depleted during the winter months ($\sim -200\%$) and enriched during the summer months ($\sim -50\%$) (Bowen and Revenaugh, 2003, Fig. 1b).

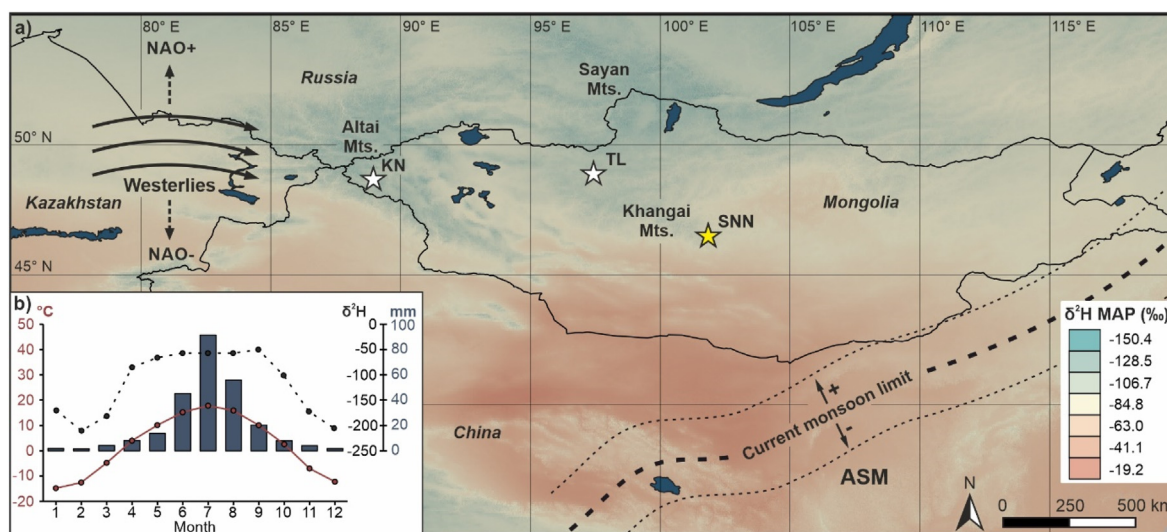


Fig. 1. (a) Overview of the study area with the $\delta^2\text{H}$ distribution of mean annual precipitation (Bowen and Revenaugh, 2003). The yellow star indicates Shireet Naiman Nuur (SNN) in the southeastern Khangai Mountains. Also indicated are the sites of Telmen Nuur (TL) and Khar Nuur (KN) (white stars), that are used for comparison, as well as the two major atmospheric circulation systems, i.e., the mid-latitude Westerlies and the low-latitude ASM, and their potential spatial changes during strengthened and weakened phases. (b) Mean monthly temperature and precipitation of the nearest climate station Arvaikheer (1813 m a.s.l.; 46.27°N ; 102.78°E ; DWD Climate Center, 2021), as well as the modern modeled monthly hydrogen isotopic composition of precipitation for the site (Bowen and Revenaugh, 2003).

The regional climate in Mongolia and the Khangai Mountains is dominated by the Siberian High during winter, leading to extremely cold and dry conditions. Water vapor backward trajectories (HYSPPLIT analyses) from the Altai Mountains suggest that precipitation is primarily supplied by the mid-latitude Westerlies, bringing moisture from the North Atlantic and the Mediterranean Sea as well as recycled moisture from the inlands of Arid Central Asia (Xu et al., 2019). The ASM plays no significant role on today's moisture and precipitation distribution in Mongolia, and only small-scale convections of recycled moisture from the monsoonal region can reach Mongolia on rare occasions (Chen et al., 2019, Fig. 1).

2.2. Lithology and chronology of the studied Shireet Naiman Nuur sediments

The investigated lake sediment core from Shireet Naiman Nuur was previously described in detail by Bliedtner et al. (2022). The 178 cm long sediment core comprises mostly layered silty sediments and consists of three lithological units (see Fig. 3 in Bliedtner et al., 2022). The laminated brownish sediments of Unit A (from 178 to 118 cm) are interrupted by two pale layers at 167 and 152 cm sediment depth. A double pale layer at 114 cm sediment depth and blackish sediments at 80 cm sediment depth interrupt the laminated brownish sediments in Unit B (from 118 to 60 cm). Another pale layer occurs in Unit C (from 60 to 0 cm) at 59 cm sediment depth and well laminated brownish sediments contain intercalated blackish sediments.

Extensive ^{14}C -dating of bulk organic carbon and terrestrial macrofossils enabled the establishment of a robust and precise chronology for the Shireet Naiman Nuur sediments (see Fig. 3 in Bliedtner et al., 2022). Bayesian age-depth modeling of the ^{14}C -dated compounds gave a modeled basal median ^{14}C -age of 7.4 ± 0.3 cal ka BP, with most ^{14}C -ages in stratigraphic order, apart from a few exceptions. The terrestrial macrofossil and organic carbon ^{14}C -ages at 80 and 79 cm sediment depth, respectively, had slight age offsets, while the terrestrial macrofossil ^{14}C -age at 29 cm sediment depth had a large age offset. Those samples are pre-aged and excluded from age-depth modeling. Based on the ^{14}C -ages, an age-depth model was established by Bayesian age modeling using the Bacon 2.3.4 package in R (Blaauw and Christen, 2011). All bulk organic carbon samples were reservoir corrected during age-depth modeling using the ^{14}C -age of the uppermost bulk organic carbon sample (0–1 cm sediment depth), which gave a conventional ^{14}C -age of 632 ± 101 years. The ^{14}C -based chronology of the Shireet Naiman Nuur sediments was further confirmed by paleomagnetic secular variation (Bliedtner et al., 2022).

2.3. Compound-specific biomarker $\delta^2\text{H}$ analyses

For biomarker analyses, free total lipids were extracted from sediments by ultrasonic extraction with dichloromethane (DCM)/methanol (MeOH) (9:1, v/v) for 15 min in three cycles. The total lipid extract was separated over aminopropyl pipette columns (Supleco, 45 μm) into fractions of different polarity. The apolar fraction including the *n*-alkanes was eluted with hexane and further purified over silver nitrate (AgNO_3 ; Supelco, 60–200 mesh) pipette columns due to coeluting compounds. Identification and quantification of the *n*-alkanes was carried out on an Agilent 7890 B gas-chromatograph equipped with an Agilent HP5MS column (30 m length, 320 μm inner diameter, 0.25 μm film thickness) and a flame ionization detector, relative to external *n*-alkane standards (*n*- C_{21} – *n*- C_{40} ; Supelco). Compound-specific hydrogen isotopes of the *n*-alkanes were analyzed using an Isoprime vision isotope ratio mass spectrometer coupled via a GC5 pyrolysis-combustion interface to a gas chromatograph (Agilent 7890 B). The GC5 operated in

pyrolysis mode for the $\delta^2\text{H}$ analyses with a chrome reactor at 1050 °C. Samples were injected splitless and measured as triplicates. The analytical precision was checked twice after nine injections by certified external *n*-alkane standards with a known isotopic composition (Arndt Schimmelmann, University of Indiana). The H^{3+} -correction factor was checked regularly and gave values of 3.41 ± 0.08 . The hydrogen isotopic composition is given in its delta notation in per mil, i.e., as $\delta^2\text{H}$ versus the Vienna Standard Mean Ocean Water (VSMOW). $\Delta_{\text{aq-terr}}$, the offset between the aquatic and terrestrial *n*-alkanes, followed the calculation of Strobel et al. (2022):

$$\Delta_{\text{aq-terr}} = 1000 * [(n - \text{C}_{23} + 1000) / (n - \text{C}_{31} + 1000) - 1]$$

3. Results

n-Alkanes are present in all 92 analyzed samples from the Shireet Naiman Nuur sediments and their compound-specific $\delta^2\text{H}$ values provide distinct changes over the past 7.4 ± 0.3 cal ka BP. $\delta^2\text{H}$ values of the terrestrial *n*- C_{31} range from -219.2 ± 1.2 to $-192 \pm 1.9\text{‰}$ and $\delta^2\text{H}$ values of the aquatic *n*- C_{23} range from -199.5 ± 2.1 to $-159.9 \pm 2.0\text{‰}$ (Fig. 2). $\delta^2\text{H}$ of the aquatic *n*- C_{23}

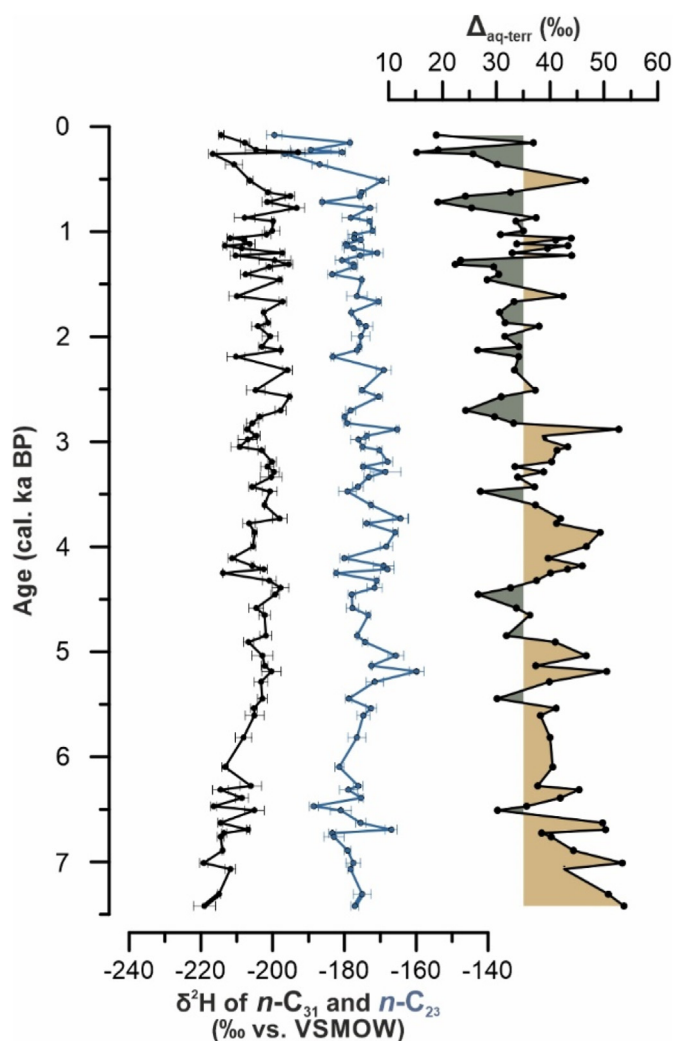


Fig. 2. Compound-specific $\delta^2\text{H}$ of the terrestrial *n*- C_{31} , the aquatic *n*- C_{23} and the isotopic offset between the aquatic and terrestrial $\delta^2\text{H}$ ($\Delta_{\text{aq-terr}}$) from the Shireet Naiman Nuur sediments.

is generally more enriched (up to ~50‰) compared to $\delta^2\text{H}$ of the terrestrial $n\text{-C}_{31}$ in the endorheic Shireet Naiman Nuur sediments, with greater enrichment from 7.4 ± 0.3 to 2.8 ± 0.2 cal ka BP and less enrichment from 2.8 ± 0.2 cal ka BP until present day. $\Delta_{\text{aq-terr}}$ is positive and ranges from 15.2 to 53.7‰ (Fig. 2). Higher values occur from 7.4 ± 0.3 to 2.8 ± 0.2 cal ka BP and become lower from 2.8 ± 0.2 cal ka BP until present day.

4. Discussion

In the Mid to Late Holocene Shireet Naiman Nuur sediments, compound-specific $\delta^2\text{H}$ values of the aquatic $n\text{-C}_{23}$ are generally more enriched compared to the terrestrial $n\text{-C}_{31}$ (up to ~50‰), and we interpret variations in the $\delta^2\text{H}$ -enrichment of the aquatic $n\text{-C}_{23}$ in terms of evaporation/precipitation changes (Fig. 2). It is notable that n -alkanes in lake sediments often contain a mixed signal from aquatic and terrestrial sources, which limit a clear determination of aquatic and terrestrial end-members and therefore the interpretation of the $\delta^2\text{H}$ signal (e.g., Yang and Bowen, 2022). However, our regional calibration studies of modern plant material, topsoils and lake surface sediments show that $n\text{-C}_{23}$ is of aquatic origin whereas $n\text{-C}_{31}$ is produced by terrestrial plants in semi-arid Mongolia (Struck et al., 2020a; Strobel et al., 2021). Moreover, we found that $\delta^2\text{H}$ of the terrestrial $n\text{-C}_{31}$ primarily records the isotopic signal of the local growing season precipitation (Struck et al., 2020b; Strobel et al., 2022), whereas $\delta^2\text{H}$ of the aquatic $n\text{-C}_{23}$ reflects the isotopic signal of the lake water used by aquatic macrophytes and algae during photosynthesis (Strobel et al., 2022). Additionally, the semi-arid Mongolian lakes, which are mostly endorheic, are highly sensitive to precipitation/evaporation changes and $\delta^2\text{H}$ of aquatic $n\text{-C}_{23}$ is often strongly enriched compared to $\delta^2\text{H}$ of the terrestrial $n\text{-C}_{31}$ indicating that lake water is strongly modified by lake water evaporation (Bliedtner et al., 2021; Strobel et al., 2022). Consequently, the isotopic offset between aquatic and terrestrial $\delta^2\text{H}$, which can be expressed as $\Delta_{\text{aq-terr}}$, is a valuable indicator for lake water evaporation and high values of $\Delta_{\text{aq-terr}}$ in the Shireet Naiman Nuur sediments from 7.4 ± 0.3 to 2.8 ± 0.2 cal ka BP indicate enhanced lake water evaporation and drier conditions. Lower $\Delta_{\text{aq-terr}}$ values from 2.8 ± 0.2 cal ka BP until present day indicate less evaporation and moister conditions at Shireet Naiman Nuur (Fig. 2).

The curves for $\Delta_{\text{aq-terr}}$ and $\log(\text{Ca/Ti})$ follow a similar pattern at Shireet Naiman Nuur and suggest that a link may exist between these records (Fig. 3b and c). We recently reported that lake primary productivity changes are reflected by $\log(\text{Ca/Ti})$ in the high-altitude Shireet Naiman Nuur sediments, which were primarily driven by ice cover periods and growing season temperatures (Bliedtner et al., 2022). The general decreasing trend in growing season temperatures from the Mid to Late Holocene at Shireet Naiman Nuur is mainly controlled by decreasing summer insolation (Fig. 3a, c). Thus, periods of enhanced evaporation and drier conditions as indicated by the $\Delta_{\text{aq-terr}}$ seem to be driven by higher growing season temperatures at Shireet Naiman Nuur, whereas periods of lower temperatures and reduced evaporation seem to promote more effective moisture at the site (Fig. 3a, b, c). Although the $\Delta_{\text{aq-terr}}$ indicates distinctively wetter conditions from 2.8 ± 0.2 cal ka BP until present day, an overall trend from drier/warmer conditions before $3.6^{+0.2}_{-0.3}$ cal ka BP to wetter/colder conditions thereafter becomes obvious when comparing $\Delta_{\text{aq-terr}}$ and $\log(\text{Ca/Ti})$ (Fig. 3b and c). This temperature dependency on lake water evaporation as observed in the Shireet Naiman Nuur sediments was only recently tested by a present-day water balance model for Telmen Nuur and also suggested for the Telmen Nuur sediments during the past ~3.8 cal ka BP (Struck et al., 2022). The 4.2 ka event, which occurs as a prominent, abrupt cooling event in the Shireet Naiman Nuur sediments at 4.2 ± 0.2 cal ka BP (Bliedtner

et al., 2022), appear exceptional as it does not follow this temperature dependency and exhibits distinctly drier conditions (Fig. 3b and c). While the cool and dry conditions are contrary to the general warm/dry and cool/wet trend at Shireet Naiman Nuur, the often acknowledged 4.2 ka cooling event has previously been reported as an extended drought event in Eurasia (see Perşoiu et al., 2019 and references therein). Cooler conditions during the 4.2 ka event are likely related to enhanced ice-rafted debris in the North Atlantic (Bond et al., 2001), which led to a strengthened and expanded Siberian High, blocking moisture from the mid-latitude Westerlies in Eurasia (Perşoiu et al., 2019). Therefore, beside the dependency with temperature, the spatial and temporal interactions of the atmospheric circulation systems have also a strong control on the hydrological conditions at Shireet Naiman Nuur and in the broader region.

The trend from drier conditions during the Mid Holocene to wetter conditions during the Late Holocene at Shireet Naiman Nuur is very well in line with a moisture index for northern central Asia compiled from multiple regional pollen, isotope and sedimentological records (Lan et al., 2021, Fig. 3b, d). However, Lan et al. (2021) suggest that temperature-induced evaporation has only minor control on regional dryness/wetness trends while the strength and latitudinal position of the mid-latitude Westerlies are strong first order controls on Holocene moisture evolution. Moreover, (in)direct influence on the past regional climate has also been attributed to the low-latitude ASM (An et al., 2008; Chen et al., 2008; Rudaya et al., 2009), and the spatial and temporal interactions between Westerlies and ASM might be crucial for understanding past hydroclimatic changes in the region.

The comparison between the Holocene moisture changes at Shireet Naiman Nuur and the intensity of the ASM recorded by $\delta^{18}\text{O}$ at Dongge Cave, which is located in the interior of monsoonal Asia, reveals a distinctly anti-correlated pattern (Fig. 3b, e; see Fig. 3i and j for location). More negative $\delta^{18}\text{O}$ values at Dongge Cave during the Mid Holocene (i.e., from ~7.5 to 3.6 cal ka BP) indicate increased precipitation amounts and an intensified ASM due to high solar summer insolation and higher sea surface temperatures. In contrast, reduced precipitation and a weakened ASM are indicated by more positive $\delta^{18}\text{O}$ values at Dongge Cave during the Late Holocene (i.e., after ~3.6 cal ka BP) due to reduced solar summer insolation and lower sea surface temperatures (Dykoski et al., 2005). This contrasts drier conditions at Shireet Naiman Nuur during the Mid Holocene and wetter conditions thereafter (Fig. 3b, e), and suggests an anti-phase relationship between our record and the ASM-dominated regions of monsoonal Asia that has previously been proposed for the Westerlies-dominated regions of central Asia and the ASM-dominated regions of monsoonal Asia (e.g., Herzschuh, 2006; Zhang and Feng, 2018; Chen et al., 2019; Xu et al., 2019). Consequently, an intensified ASM during the Mid Holocene led to a northward displacement of the monsoonal limit, and the adjacent subsidence dry zones north of the monsoonal limit likewise intensified and shifted northwards as schematically illustrated in Fig. 3j. While the monsoonal limit is presently located south of Mongolia, a proposed northward shift of ~400 km during the Mid Holocene (Goldsmith et al., 2017) will very likely result in a displacement of the subsidence dry zones over Central Mongolia and the Khangai Mountains (Figs. 1 and 3j). This displacement of the subsidence dry zones to the north would have led to increased dryness at Shireet Naiman Nuur because moisture-bearing Westerlies were prevented from penetrating into the region. Decreasing summer insolation and a weakened ASM during the Late Holocene resulted in a southward shift of the monsoonal limit and the adjacent subsidence dry zones, allowing the Westerlies to control the overall wetter climate in central Mongolia by changes in its strength and latitudinal position on millennial to decadal

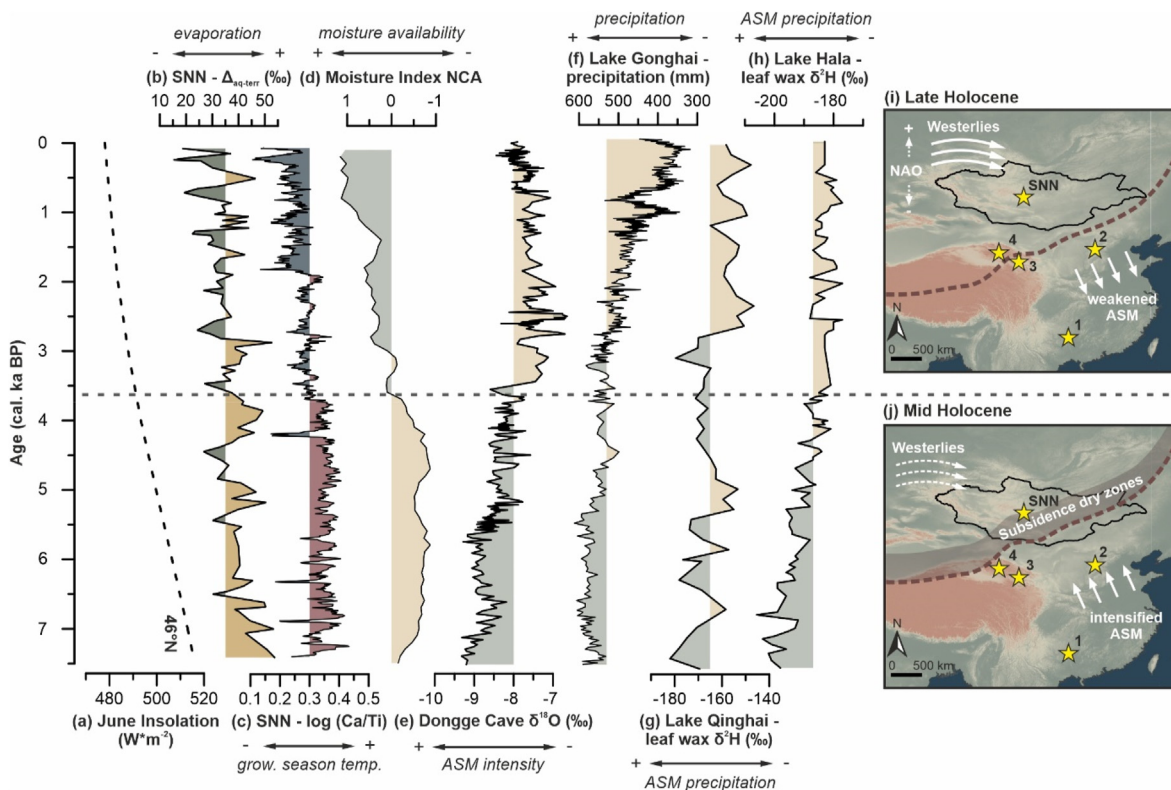


Fig. 3. Anti-phase relationship between the moisture evolution of semi-arid Mongolia and monsoonal Asia. Comparison of (b) Holocene moisture changes at Shireet Naiman Nuur (SNN; $\Delta_{aq-terr}$) with (a) June insolation at the site latitude (46°N) (Laskar et al., 2004), (c) log (Ca/Ti) from Shireet Naiman Nuur (Bliedtner et al., 2022), (d) a multi-proxy-based moisture index from northern Central Asia (Lan et al., 2021), (e) $\delta^{18}\text{O}$ from Dongge Cave (Dykoski et al., 2005), (f) pollen-based precipitation reconstruction from Lake Gonghai (Ding et al., 2017), (g) leaf wax $\delta^2\text{H}$ of *n*-alkanoic acid C_{28} from Lake Qinghai (Thomas et al., 2016) and (h) leaf wax $\delta^2\text{H}$ of *n*-alkane C_{31} from Lake Hala (Aichner et al., 2022). The assumed spatial evolution of the major atmospheric circulation systems, i.e., the Westerlies and ASM, during the Late and Mid Holocene are illustrated in (i) and (j). The numbers in (i) and (j) refer to the locations of the paleoclimate records used for comparison: 1 = Dongge Cave, 2 = Lake Gonghai, 3 = Lake Qinghai and 4 = Lake Hala.

timescales (Routson et al., 2019; Lan et al., 2021, Fig. 3i). This decreasing trend of the ASM intensity from the Mid to the Late Holocene is also recorded by speleothem $\delta^{18}\text{O}$ records from the interior of monsoonal Asia (see stacked $\delta^{18}\text{O}$ record from Yang et al., 2019), and a likewise decreasing trend of ASM-related precipitation is shown by multiple lacustrine records from the monsoonal realm, even by those records located near the present monsoon limit. This trend is illustrated in Fig. 3 by a pollen-based precipitation reconstruction from Lake Gonghai (Chen et al., 2015, Fig. 3f), and two leaf wax $\delta^2\text{H}$ records from Lake Qinghai (Thomas et al., 2016, Fig. 3g) and Lake Hala (Aichner et al., 2022, Fig. 3h), all showing an anti-phased moisture pattern to the Shireet Naiman Nuur record (Fig. 3b). In contrast, Mid Holocene dryness is often reported from lake sediment records in Westerlies-influenced Central Asia and Mongolia (Fowell et al., 2003; Prokopenko et al., 2007; Schwanghart et al., 2009; Wang et al., 2011; Lan et al., 2021) further supporting our paleohydrological findings from Shireet Naiman Nuur and the distinct anti-phase relationship of dryness/wetness trends between Central Asia, including Mongolia, and monsoonal Asia. Moreover, the influence of the spatial pattern and interaction of the Westerlies and the EASM plays an important role on regional hydrological conditions.

Generally wetter conditions during the past ~ 3.6 cal ka BP at Shireet Naiman Nuur correspond well with the suggested increasing predominance of the mid-latitude Westerlies on Central Asia's hydrology during the Late Holocene. Interruptions of the overall wetter conditions at Shireet Naiman Nuur by drier conditions at ~ 3 , ~ 1.5 , ~ 1 and 0.5 cal ka BP further suggest that short-term fluctuations in hydrological conditions are probably related to the

strength and latitudinal position of the Westerlies (Chen et al., 2019; Lan et al., 2021). This pattern of overall wetter conditions during the last 3.6 cal ka BP interrupted by short-term periods of dry conditions is in good agreement with hydrological variations recorded by an evaporation index (EI) in a lake sediment record from Telmen Nuur (Struck et al., 2022) also located in Central Mongolia ~ 400 km northwest of Shireet Naiman Nuur (see Fig. 1 for location). Phases of wetter and drier conditions are especially well matched in both records during the last ~ 2.8 cal ka BP (Fig. 4a and b). Differences between both records exist before ~ 2.8 cal ka BP, especially the timing of the dry phase at ~ 3.5 cal ka BP at Telmen Nuur could potentially correspond to the dry phase at ~ 3.8 cal ka BP at Shireet Naiman Nuur due to chronological uncertainties in the Telmen Nuur sediments during the period from ~ 3.6 to 3.0 cal ka BP. However, those differences are still within both chronologies 2σ uncertainties. Comparison of hydrological changes at Shireet Naiman Nuur and Telmen Nuur with the North Atlantic Oscillation (NAO) index (Faust et al., 2016) indicates that wetter conditions at both sites very well correspond with negative NAO phases (Fig. 4a, b, c). During negative NAO phases, the Westerlies are displaced southward because of northern hemispheric cooling and a greater latitudinal temperature and pressure gradient between the Sub-tropical High and Subpolar Low in the North Atlantic (Olsen et al., 2012; Faust et al., 2016). It has been suggested that moisture and precipitation, and especially precipitation during late winter/early spring, is increasingly brought to Central Asia and Mongolia during negative NAO phases, with moisture being mainly advected from the southern part of the North Atlantic and the Mediterranean Sea (Aizen et al., 2001; Yang et al., 2020). This relationship of higher

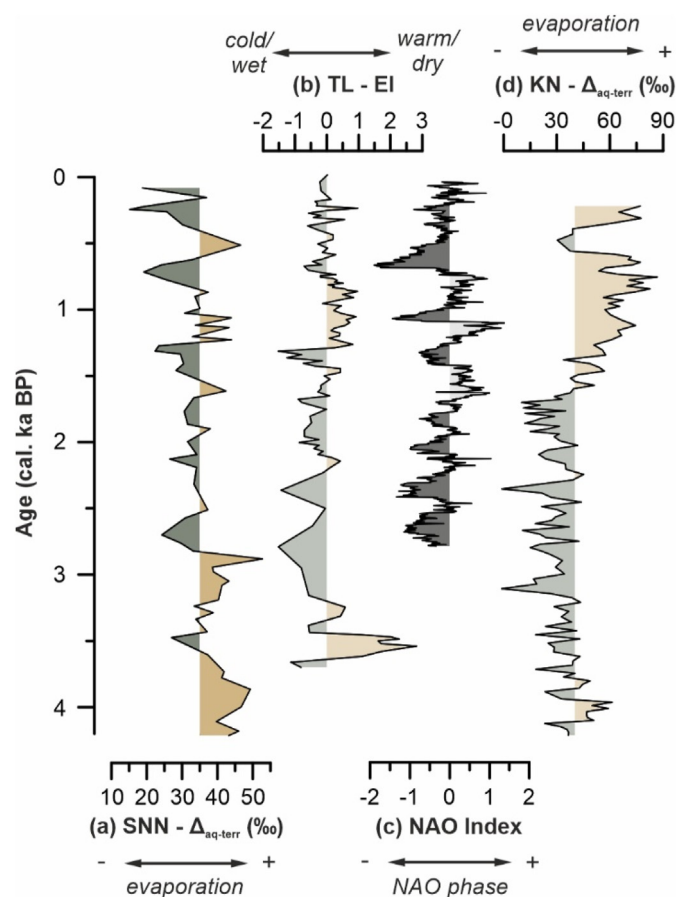


Fig. 4. Short-term hydrological fluctuations during the Late Holocene. Comparison of (a) Holocene moisture changes at Shireet Naiman Nuur (SNN; $\Delta_{\text{aq-terr}}$) with (b) an isotope-based evaporation index (EI) from Telmen Nuur (TL; Struck et al., 2022), (c) a North Atlantic Oscillation (NAO) Index (Faust et al., 2016) and (d) $\Delta_{\text{aq-terr}}$ from Khar Nuur (KN; Bliedtner et al., 2021).

precipitation during negative NAO phases is further supported by modeled modern water vapor backward trajectories from the Tian Shan/Pamir Mountains (Wolff et al., 2017; Yan et al., 2019) and the Altai Mountains (Xu et al., 2019). In contrast, drier conditions and less precipitation seem to occur in central Mongolia and at Shireet Naiman Nuur during positive NAO phases (i.e., at ~ 3 , ~ 1.5 , ~ 1 and 0.5 cal ka BP; Fig. 4a, c), because warming and lower temperature gradients in the North Atlantic led to a displacement of the Westerlies further north. Therefore, precipitation and moisture availability at Shireet Naiman Nuur is mostly related to the latitudinal position of the Westerlies driven by the NAO. However, following the discussion about $\log(\text{Ca}/\text{Ti})$ in the Shireet Naiman Nuur sediments above, temperature also plays an important role on regional hydrological changes and is highly linked with the position of the Westerlies during the Late Holocene. This is because the position of the Westerlies is related to temperature and pressure gradients in the northern hemisphere and moisture-bearing Westerlies co-occur with lower temperatures and reduced evaporation during negative NAO phases and vice versa.

Overall, the Late Holocene moisture pattern at Shireet Naiman Nuur resembles existing records in central Mongolia, e.g., Khuisiin Nuur (Tian et al., 2013), Bayan Nuur (Yang et al., 2020) and Telmen Nuur (Struck et al., 2022), suggesting Westerlies and temperature as the dominant forcing mechanisms on regional hydrology. Comparing central Mongolia to the Mongolian Altai, a mostly

similar Late Holocene moisture pattern can be observed at Khar Nuur (Bliedtner et al., 2021), although the magnitude of evaporation changes in the Khar Nuur catchment (i.e., changes in $\Delta_{\text{aq-terr}}$) is different (Fig. 4d). In particular, an exceptionally strong evaporative enrichment and increased dryness occurred in the Khar Nuur catchment from ~ 1.5 to 0.5 cal ka BP, which are absent at Shireet Naiman Nuur and in other records in central Mongolia. However, those differences might be explained by the slightly different environmental settings in the Altai Mountains with even colder temperatures and less precipitation at Khar Nuur as observed today (Bliedtner et al., 2021). Khar Nuur is additionally located in the eastern part of the Altai Mountains with a greater influence of rain-shadow effects, and the lake therefore probably reacts to a much greater degree to changes in precipitation versus evaporation than the central Mongolian lakes. Despite slight differences, the Khar Nuur hydrological record mostly follows our hydrological reconstruction from Shireet Naiman Nuur.

5. Conclusions

Our study investigated the Mid to Late Holocene moisture evolution in semi-arid central Mongolia by compound-specific biomarker $\delta^2\text{H}$ analyzes of the 7.4 cal ka long lake sediment sequence from Shireet Naiman Nuur. $\Delta_{\text{aq-terr}}$, our hydrological indicator for evaporation changes in a lake catchment, closely resembles our previously published changes in growing season temperatures, indicating an overall trend of increased evaporation and drier/warmer conditions at Shireet Naiman Nuur from ~ 7.4 to ~ 3.6 cal ka BP (i.e., during the Mid Holocene). Reduced evaporation and wetter/colder conditions occurred thereafter (i.e., ~ 3.6 cal ka BP until present day; during the Late Holocene). While moisture availability at Shireet Naiman Nuur seems to be related to changes in temperature and evaporation, the spatial pattern and interaction of the mid-latitude Westerlies and low-latitude ASM also exert important control on regional precipitation and moisture changes. From the Mid to Late Holocene, a strong anti-phasing of our record with records from monsoonal Asia suggest that an intensified ASM displaced the monsoonal limit northward during the Mid Holocene. The adjacent subsidence dry zones were likewise shifted northwards over central Mongolia, preventing moisture supply into the region and leading to drier conditions. A weakened ASM and southward displacement of the monsoonal limit during the Late Holocene allowed the moisture-bearing Westerlies to penetrate into central Mongolia leading to wetter conditions. Short-term hydrological fluctuations of the overall wet conditions at Shireet Naiman Nuur and central Mongolia during the Late Holocene are determined by the strength and latitudinal position of the Westerlies. Increased precipitation and moisture availability occur during negative NAO phases where the Westerlies are shifted southwards and bring more precipitation from the southern Atlantic and Mediterranean Sea during late winter/spring. Short-term drier conditions with less precipitation occur during positive NAO phases because the Westerlies are shifted north of central Mongolia.

CRedit authorship contribution statement

Marcel Bliedtner: Conceptualization, Formal analysis, Funding acquisition, Investigation, Writing – original draft. **Paul Strobel:** Conceptualization, Investigation, Writing – review & editing. **Julian Struck:** Conceptualization, Writing – review & editing. **Maximilian Prochnow:** Investigation, Writing – review & editing. **Enkhtuya Bazarradnaa:** Writing – review & editing. **Roland Zech:** Conceptualization, Writing – review & editing.

Declaration of competing interest

The authors declare that they have no known competing financial interests or personal relationships that could have appeared to influence the work reported in this paper.

Data availability

The data presented in this study are included in the Supporting Material

Acknowledgments

This study was funded by the German Research Foundation DFG (BL 1781/2–1). We would like to thank the Ernst Abbe Stiftung for financial support of the field trip to Mongolia and sediment retrieval. We further thank our logistic partners in Mongolia for their support during fieldwork and all participants of the field campaign in 2019. M. Prochnow acknowledges the support by a fellowship from the federal state of Thuringia (Landesgraduiertenstipendium). Especially acknowledged are J. Lohrlein and M. Wagner for support during laboratory work. We thank three reviewers for their valuable and helpful comments on this paper.

Appendix A. Supplementary data

Supplementary data to this article can be found online at <https://doi.org/10.1016/j.quascirev.2023.108201>.

References

- Aichner, B., Makhmudov, Z., Rajabov, I., Zhang, Q., Pausata, F.S.R., Werner, M., et al., 2019. Hydroclimate in the pamirs was driven by changes in precipitation–evaporation seasonality since the last glacial period. *Geophys. Res. Lett.* 46 (23), 13972–13983. <https://doi.org/10.1029/2019GL085202>.
- Aichner, B., Wünnemann, B., Callegaro, A., van der Meer, M.T.J., Yan, D., Zhang, Y., Barbante, C., Sachse, D., 2022. Asynchronous responses of aquatic ecosystems to hydroclimatic forcing on the Tibetan Plateau. *Commun Earth Environ* 3 (1). <https://doi.org/10.1038/s43247-021-00325-1>.
- Aizen, E.M., Aizen, V.B., Melack, J.M., Nakamura, T., Ohta, T., 2001. Precipitation and atmospheric circulation patterns at mid-latitudes of Asia. *Int. J. Climatol.* 21 (5), 535–556. <https://doi.org/10.1002/joc.626>.
- An, C.-B., Chen, F.-H., Barton, L., 2008. Holocene environmental changes in Mongolia: a review. *Global Planet. Change* 63 (4), 283–289. <https://doi.org/10.1016/j.gloplacha.2008.03.007>.
- Blaauw, M., Christen, J.A., 2011. Flexible paleoclimate age-depth models using an autoregressive gamma process. *Bayesian Analysis* 6 (3), 457–474. <https://doi.org/10.1214/11-BA618>.
- Bliedtner, M., Strobel, P., Struck, J., Salazar, G., Szidat, S., Nowaczyk, N., et al., 2022. Holocene temperature variations in semi-arid Central Mongolia—a chronological and sedimentological perspective from a 7400-year lake sediment record from the Khangai Mountains. *Front. Earth Sci.* 10. <https://doi.org/10.3389/feart.2022.910782>.
- Bliedtner, M., Struck, J., Strobel, P., Salazar, G., Szidat, S., Bazarradnaa, E., et al., 2021. Late holocene climate changes in the Altai region based on a first high-resolution biomarker isotope record from Lake khar Nuur. *Geophys. Res. Lett.* 48 (20). <https://doi.org/10.1029/2021GL094299>.
- Bond, G., Kromer, B., Beer, J., Muscheler, R., Evans, M.N., Showers, W., et al., 2001. Persistent solar influence on North Atlantic climate during the holocene. *Science* 294 (5549), 2130–2136. <https://doi.org/10.1126/science.1065680>.
- Bowen, G.J., Revenaugh, J., 2003. Interpolating the isotopic composition of modern meteoric precipitation. *Water Resour. Res.* 39 (10). <https://doi.org/10.1029/2003WR002086> n/a–n/a.
- Chen, F., Chen, J., Huang, W., Chen, S., Huang, X., Jin, L., et al., 2019. Westerlies Asia and monsoonal Asia: spatiotemporal differences in climate change and possible mechanisms on decadal to sub-orbital timescales. *Earth Sci. Rev.* 192, 337–354. <https://doi.org/10.1016/j.earscirev.2019.03.005>.
- Chen, F., Xu, Q., Chen, J., Birks, H.J.B., Liu, J., Zhang, S., et al., 2015. East Asian summer monsoon precipitation variability since the last deglaciation. *Sci. Rep.* 5, 11186. <https://doi.org/10.1038/srep11186>.
- Chen, F., Yu, Z., Yang, M., Ito, E., Wang, S., Madsen, D.B., et al., 2008. Holocene moisture evolution in arid central Asia and its out-of-phase relationship with Asian monsoon history. *Quat. Sci. Rev.* 27 (3–4), 351–364. <https://doi.org/10.1016/j.quascirev.2007.10.017>.
- D'Arrigo, R., Jacoby, G., Pederson, N., Frank, D., Buckley, B., Nachin, B., et al., 2000. Mongolian tree-rings, temperature sensitivity and reconstructions of Northern Hemisphere temperature. *Holocene* 10 (6), 669–672. <https://doi.org/10.1191/09596830094926>.
- Dykoski, C., Edwards, R., Cheng, H., Yuan, D., Cai, Y., Zhang, M., et al., 2005. A high-resolution, absolute-dated Holocene and deglacial Asian monsoon record from Dongge Cave, China. *Earth Planet Sci. Lett.* 233 (1–2), 71–86. <https://doi.org/10.1016/j.epsl.2005.01.036>.
- Faust, J.C., Fabian, K., Milzer, G., Giraudeau, J., Knies, J., 2016. Norwegian fjord sediments reveal NAO related winter temperature and precipitation changes of the past 2800 years. *Earth Planet Sci. Lett.* 435, 84–93. <https://doi.org/10.1016/j.epsl.2015.12.003>.
- Fowell, S.J., Hansen, B.C., Peck, J.A., Khosbayan, P., Ganbold, E., 2003. Mid to late holocene climate evolution of the lake telmen basin, north central Mongolia, based on palynological data. *Quat. Res.* 59 (3), 353–363. [https://doi.org/10.1016/S0033-5894\(02\)00020-0](https://doi.org/10.1016/S0033-5894(02)00020-0).
- Ficken, K., Li, B., Swain, D., Eglinton, G., 2000. An n-alkane proxy for the sedimentary input of submerged/floating freshwater aquatic macrophytes. *Org. Geochem.* 31 (7–8), 745–749. [https://doi.org/10.1016/S0146-6380\(00\)00081-4](https://doi.org/10.1016/S0146-6380(00)00081-4).
- Goldsmith, Y., Broecker, W.S., Xu, H., Polissar, P.J., deMenocal, P.B., Porat, N., et al., 2017. Northward extent of East Asian monsoon covaries with intensity on orbital and millennial timescales. *Proc. Natl. Acad. Sci. U. S. A.* 114 (8), 1817–1821. <https://doi.org/10.1073/pnas.1616708114>.
- Gunin, P.D., Vostokova, E.A., Dorofeyuk, N.I., Tarasov, P.E., Black, C.C., 1999. *Vegetation Dynamics of Mongolia*. Springer Netherlands, Dordrecht.
- Herzschuh, U., 2006. Palaeo-moisture evolution in monsoonal Central Asia during the last 50,000 years. *Quat. Sci. Rev.* 25 (1–2), 163–178. <https://doi.org/10.1016/j.quascirev.2005.02.006>.
- Hessl, A.E., Anchukaitis, K.J., Jelsema, C., Cook, B., Byambasuren, O., Leland, C., et al., 2018. Past and future drought in Mongolia. *Sci. Adv.* 4 (3), e1701832. <https://doi.org/10.1126/sciadv.1701832>.
- Hoerling, M.P., Hurrell, J.W., Xu, T., 2001. Tropical origins for recent North Atlantic climate change. *Science (New York, N.Y.)* 292 (5514), 90–92. <https://doi.org/10.1126/science.1058582>.
- IPCC, 2021. *Climate Change 2021: the Physical Science Basis. Contribution of Working Group I to the Sixth Assessment Report of the Intergovernmental Panel on Climate Change*. Cambridge University Press, Cambridge, UK.
- Klinge, M., Sauer, D., 2019. Spatial pattern of Late Glacial and Holocene climatic and environmental development in Western Mongolia - a critical review and synthesis. *Quat. Sci. Rev.* 210, 26–50. <https://doi.org/10.1016/j.quascirev.2019.02.020>.
- Lan, J., Wang, T., Dong, J., Kang, S., Cheng, P., Zhou, K., et al., 2021. The influence of ice sheet and solar insolation on Holocene moisture evolution in northern Central Asia. *Earth Sci. Rev.* 217, 103645. <https://doi.org/10.1016/j.earscirev.2021.103645>.
- Marin, A., 2010. Riders under storms: contributions of nomadic herders' observations to analysing climate change in Mongolia. *Global Environ. Change* 20 (1), 162–176. <https://doi.org/10.1016/j.gloenvcha.2009.10.004>.
- Mohtadi, M., Prange, M., Steinke, S., 2016. Palaeoclimatic insights into forcing and response of monsoon rainfall. *Nature* 533 (7602), 191–199. <https://doi.org/10.1038/nature17450>.
- Mügler, I., Sachse, D., Werner, M., Xu, B., Wu, G., Yao, T., Gleixner, G., 2008. Effect of lake evaporation on δD values of lacustrine n-alkanes: a comparison of Nam Co (Tibetan Plateau) and Holzmaar (Germany). *Org. Geochem.* 39 (6), 711–729. <https://doi.org/10.1016/j.orggeochem.2008.02.008>.
- Nanzad, L., Zhang, J., Tuvdendorj, B., Yang, S., Rinzin, S., Prodhon, F.A., Sharma, T.P.P., 2021. Assessment of drought impact on net primary productivity in the terrestrial ecosystems of Mongolia from 2003 to 2018. *Rem. Sens.* 13 (13), 2522. <https://doi.org/10.3390/rs1313252>.
- Olsen, J., Anderson, N.J., Knudsen, M.F., 2012. Variability of the North Atlantic oscillation over the past 5,200 years. *Nat. Geosci.* 5 (11), 808–812. <https://doi.org/10.1038/ngeo1589>.
- Perşoiu, A., Ionita, M., Weiss, H., 2019. Atmospheric blocking induced by the strengthened Siberian High led to drying in west Asia during the 4.2 ka BP event – a hypothesis. *Clim. Past* 15 (2), 781–793. <https://doi.org/10.5194/cp-15-781-2019>.
- Prokopenko, A.A., Khursevich, G.K., Bezrukova, E.V., Kuzmin, M.I., Boes, X., Williams, D.F., Fedenya, S.A., Kulagina, N.V., Letunova, P.P., Abzaeva, A.A., 2007. Paleo-environmental proxy records from Lake Hovsgol, Mongolia, and a synthesis of Holocene climate change in the Lake Baikal watershed. *Quat. Res.* 68 (1), 2–17. <https://doi.org/10.1016/j.yqres.2007.03.008>.
- Routson, C.C., McKay, N.P., Kaufman, D.S., Erb, M.P., Goosse, H., Shuman, B.N., et al., 2019. Mid-latitude net precipitation decreased with Arctic warming during the Holocene. *Nature* 568 (7750), 83–87. <https://doi.org/10.1038/s41586-019-1060-3>.
- Rudaya, N., Tarasov, P., Dorofeyuk, N., Solovieva, N., Kalugin, I., Andreev, A., et al., 2009. Holocene environments and climate in the Mongolian Altai reconstructed from the Hoton-Nur pollen and diatom records: a step towards better understanding climate dynamics in Central Asia. *Quat. Sci. Rev.* 28 (5–6), 540–554. <https://doi.org/10.1016/j.quascirev.2008.10.013>.
- Sachse, D., Radke, J., Gleixner, G., 2004. Hydrogen isotope ratios of recent lacustrine sedimentary n-alkanes record modern climate variability. *Geochem. Cosmochim. Acta* 68 (23), 4877–4889. <https://doi.org/10.1016/j.gca.2004.06.004>.
- Sachse, D., Billault, I., Bowen, G.J., Chikaraishi, Y., Dawson, T.E., Feakins, S.J., et al., 2012. Molecular paleohydrology: interpreting the hydrogen-isotopic

- composition of lipid biomarkers from photosynthesizing organisms. *Annu. Rev. Earth Planet. Sci.* 40 (1), 221–249. <https://doi.org/10.1146/annurev-earth-042711-105535>.
- Schwanghart, W., Frechen, M., Kuhn, N.J., Schütt, B., 2009. Holocene environmental changes in the Ugii Nuur basin, Mongolia. *Palaeogeogr. Palaeoclimatol. Palaeoecol.* 279 (3–4), 160–171. <https://doi.org/10.1016/j.palaeo.2009.05.007>.
- Strobel, P., Struck, J., Zech, R., Bliedtner, M., 2021. The spatial distribution of sedimentary compounds and their environmental implications in surface sediments of Lake Khar Nuur (Mongolian Altai). *Earth Surf. Process. Landforms* 46 (3), 611–625. <https://doi.org/10.1002/esp.5049>.
- Strobel, P., Struck, J., Bazarradnaa, E., Zech, M., Zech, R., Bliedtner, M., 2022. Precipitation and Lake water evaporation recorded by terrestrial and aquatic n-alkane $\delta^2\text{H}$ isotopes in lake Khar Nuur, Mongolia. *G-cubed* 23 (2). <https://doi.org/10.1029/2021GC010234>.
- Struck, J., Bliedtner, M., Strobel, P., Schumacher, J., Bazarradnaa, E., Zech, R., 2020a. Leaf wax n-alkane patterns and compound-specific $\delta^{13}\text{C}$ of plants and topsoils from semi-arid and arid Mongolia. *Biogeosciences* 17 (3), 567–580. <https://doi.org/10.5194/bg-17-567-2020>.
- Struck, J., Bliedtner, M., Strobel, P., Bittner, L., Bazarradnaa, E., Andreeva, D., et al., 2020b. Leaf waxes and hemicelluloses in topsoils reflect the $\delta^2\text{H}$ and $\delta^{18}\text{O}$ isotopic composition of precipitation in Mongolia. *Front. Earth Sci.* 8. <https://doi.org/10.3389/feart.2020.00343>.
- Struck, J., Bliedtner, M., Strobel, P., Taylor, W., Biskop, S., Plessen, B., et al., 2022. Central Mongolian lake sediments reveal new insights on climate change and equestrian empires in the Eastern Steppes. *Sci. Rep.* 12 (1). <https://doi.org/10.1038/s41598-022-06659-w>.
- Sun, A., Feng, Z., Ran, M., Zhang, C., 2013. Pollen-recorded bioclimatic variations of the last ~22,600 years retrieved from Achit Nuur core in the western Mongolian Plateau. *Quat. Int.* 311, 36–43. <https://doi.org/10.1016/j.quaint.2013.07.002>.
- Thomas, E.K., Huang, Y., Clemens, S.C., Colman, S.M., Morrill, C., Wegener, P., Zhao, J., 2016. Changes in dominant moisture sources and the consequences for hydroclimate on the northeastern Tibetan Plateau during the past 32 yr. *Quat. Sci. Rev.* 131, 157–167. <https://doi.org/10.1016/j.quascirev.2015.11.003>.
- Tian, F., Herzsich, U., Dallmeyer, A., Xu, Q., Mischke, S., Biskaborn, B.K., 2013. Environmental variability in the monsoon–westerlies transition zone during the last 1200 years: lake sediment analyses from central Mongolia and supra–regional synthesis. *Quat. Sci. Rev.* 73, 31–47. <https://doi.org/10.1016/j.quascirev.2013.05.005>.
- Unkelbach, J., Kashima, K., Enters, D., Dulamsuren, C., Punsalpaamuu, G., Behling, H., 2019. Late Holocene (Meghalayan) palaeoenvironmental evolution inferred from multi-proxy-studies of lacustrine sediments from the Dayan Nuur region of Mongolia. *Palaeogeogr. Palaeoclimatol. Palaeoecol.* 530, 1–14. <https://doi.org/10.1016/j.palaeo.2019.05.021>.
- Wang, W., Ma, Y., Feng, Z., Narantsetseg, T., Liu, K.-B., Zhai, X., 2011. A prolonged dry mid-Holocene climate revealed by pollen and diatom records from Lake Ugii Nuur in central Mongolia. *Quat. Int.* 229 (1–2), 74–83. <https://doi.org/10.1016/j.quaint.2010.06.005>.
- Wang, W., Feng, Z., 2013. Holocene moisture evolution across the Mongolian Plateau and its surrounding areas: a synthesis of climatic records. *Earth Sci. Rev.* 122, 38–57. <https://doi.org/10.1016/j.earscirev.2013.03.005>.
- Wolff, C., Plessen, B., Dudashvili, A.S., Breitenbach, S.F.M., Cheng, H., Edwards, L.R., Strecker, M.R., 2017. Precipitation evolution of Central Asia during the last 5000 years. *Holocene* 27 (1), 142–154. <https://doi.org/10.1177/0959683616652711>.
- Xia, Z.-H., Xu, B.-Q., Mügler, I., Wu, G.-J., Gleixner, G., Sachse, D., Zhu, L.-P., 2008. Hydrogen isotope ratios of terrigenous n-alkanes in lacustrine surface sediment of the Tibetan Plateau record the precipitation signal. *Geochem. J.* 42 (4), 331–338. <https://doi.org/10.2343/geochemj.42.331>.
- Xu, H., Zhou, K., Lan, J., Zhang, G., Zhou, X., 2019. Arid Central Asia saw mid-Holocene drought. *Geology* 47 (3), 255–258. <https://doi.org/10.1130/G45686.1>.
- Yan, D., Xu, H., Lan, J., Zhou, K., Ye, Y., Zhang, J., et al., 2019. Solar activity and the westerlies dominate decadal hydroclimatic changes over arid Central Asia. *Global Planet. Change* 173, 53–60. <https://doi.org/10.1016/j.gloplacha.2018.12.006>.
- Yang, D., Bowen, G.J., 2022. Integrating plant wax abundance and isotopes for paleovegetation and paleoclimate reconstructions: a multi-source mixing model using a Bayesian framework. *Clim. Past* 18 (10), 2181–2210. <https://doi.org/10.5194/cp-18-2181-2022>.
- Yang, X., Yang, H., Wang, B., Huang, L.-J., Shen, C.-C., Edwards, R.L., Cheng, H., 2019. Early-Holocene monsoon instability and climatic optimum recorded by Chinese stalagmites. *Holocene* 29 (6), 1059–1067. <https://doi.org/10.1177/0959683619831433>.
- Yang, Y., Ran, M., Sun, A., 2020. Pollen-recorded bioclimatic variations of the last ~2000 years retrieved from Bayan Nuur in the western Mongolian Plateau. *Boreas* 49 (2), 350–362. <https://doi.org/10.1111/bor.12423>.
- Zhang, D., Feng, Z., 2018. Holocene climate variations in the Altai Mountains and the surrounding areas: a synthesis of pollen records. *Earth Sci. Rev.* 185, 847–869. <https://doi.org/10.1016/j.earscirev.2018.08.007>.